

Brain Oxygen Utilization Measured with O-15 Radiotracers and Positron Emission Tomography

M. A. Mintun, M. E. Raichle, W. R. W. Martin, and P. Herscovitch

The Edward Mallinckrodt Institute of Radiology, The McDonnell Center for Studies of Higher Brain Function, and Washington University School of Medicine, St. Louis, Missouri

We have developed, implemented, and validated a method for the measurement of the local cerebral metabolic rate for oxygen (CMRO₂) with positron emission tomography (PET). We use data from a single inhalation of O-15-labeled CO for cerebral blood volume (CBV), an intravenous injection of [O-15]H₂O for cerebral blood flow (CBF), and a single inhalation of [O-15]O₂ for the final calculation of CMRO₂ and the extraction of oxygen (E). The mathematical model used to analyze the data consists of two compartments and accounts for production and egress of water of metabolism in the tissue, recirculating water of metabolism, and the arterial, venous, and capillary contents of [O-15]O₂ in the brain. We validated our technique in baboons by comparing the PET-measured E with E measured using an intracarotid injection of [O-15]O₂. The correlation between these two techniques was excellent. Mathematical simulations were done to examine the effect of errors in CBV, CBF, and recirculating water of metabolism on the measurement of E and CMRO₂. The technique was implemented on five normal human subjects in whom the global CMRO₂ was 2.93 ± 0.37 (s.d.) ml/min·100 g.

J Nucl Med 25: 177-187, 1984

The introduction of molecular oxygen-15 ($T_{1/2} = 123$ sec) into the vascular compartment of the body results in the distribution of the labeled oxygen to the tissues, where it is converted to O-15-labeled water of metabolism. The labeled water then redistributes to all tissues by way of the same vascular compartment. Unmetabolized labeled molecular oxygen is ultimately removed by respiration.

These properties of the oxygen-15 tracer have been incorporated into an equilibrium model that has been used to measure oxygen consumption in the human brain using data from the sequential inhalation to equilibrium of [O-15]oxygen and carbon dioxide (1,2). Important disadvantages of this technique include the relatively complex system required for constant delivery of the

radiolabeled gases, and the long scan times during which, it is assumed, no change in physiologic state occurs.

Previous data from our laboratory (3,4) demonstrate that, after the direct intracarotid injection of a small aliquot of blood labeled with oxygen-15 into laboratory animals and humans, one can use a knowledge of the biological behavior of the tracer to analyze the externally detected time-activity curve and compute accurately the net extraction of oxygen by the brain. Positron emission tomography (PET), despite recent improvements that permit temporal resolution of less than 1 min, does not have the sensitivity to describe a time-activity curve with enough accuracy to implement this technique as initially described (3) and validated (4). Furthermore, this technique assumes that all tracer administered is present initially in the desired region of interest—i.e., that the input is a delta function. This can be obtained for the brain only with a direct injection of the internal carotid, with a resultant image of only one cerebral hemisphere.

Received Mar. 8, 1983; revision accepted Sept. 9, 1983.

For reprints contact: M. E. Raichle, MD, Box 8131, Washington University School of Medicine, St. Louis, MO 63110.

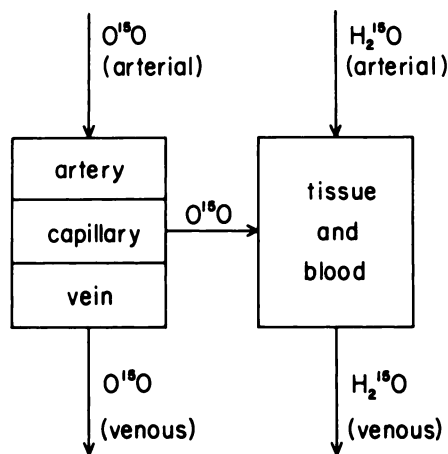


FIG. 1. Two-compartment model chosen to analyze behavior of two O-15 radiotracers, $O^{15}O$ and $H_2^{15}O$. Left compartment represents $O^{15}O$ in vascular spaces; right compartment represents water of metabolism, $H_2^{15}O$, in tissue and blood spaces. Each compartment has separate entrance and exit of tracer, interacting with each other only through extraction of $O^{15}O$ from vascular space and subsequent conversion to water of metabolism.

This method of tracer administration is not in keeping with the purpose of PET, which strives for safety of administration by intravenous injection or inhalation. Our approach to measurement of local cerebral oxygen consumption accommodates these issues, and is outlined below.

We developed a compartmental model to describe the behavior of oxygen-15-labeled molecular oxygen and water of metabolism simultaneously in the brain. The model is used to calculate local cerebral utilization rate of oxygen ($CMRO_2$) and oxygen extraction (E), given the local blood flow, the local blood volume, and the

oxygen-15 activity in arterial blood and brain tissue following an inhalation of O-15 oxygen gas. Operationally, the brain tissue activity is measured with a single PET scan and the values for blood volume and blood flow are obtained by techniques requiring a separate tracer administration and PET scan.

MATERIALS AND METHODS

Model. The schematic and symbols of the oxygen-15 model are presented in Fig. 1 and Table 1, respectively.

The model assumes only two compartments for oxygen-15 corresponding to the different molecular forms, $O^{15}O$ and $H_2^{15}O$, found in the brain. The first compartment, containing $O^{15}O$, corresponds physically to the intravascular space. The molecular oxygen enters through arterial input and leaves through venous drainage. It is assumed that the diffusion of $O^{15}O$ into the tissue space can be expressed by a fractional extraction, E , specific for a given region, times the arterial input. Once in the vascular space, the $O^{15}O$ is assumed to be metabolized immediately to $H_2^{15}O$, and enters the second compartment. Thus, the oxygen content of the extravascular tissue is assumed to be zero (see Discussion for further comments on this assumption).

The second compartment for $H_2^{15}O$ physically corresponds to the distribution space for free water in the brain, including all vascular spaces. The entrance of tracer occurs from arterial input redistributing $H_2^{15}O$ from all tissues, and from $H_2^{15}O$ of metabolism created locally. The latter amount is, of course, equal to the local extraction fraction times the $O^{15}O$ arterial input curve as described above. The exit of $H_2^{15}O$ occurs by venous

TABLE 1. VARIABLES USED IN THE PET OXYGEN MODEL

Symbol	Description	Units
V_i	Volume of compartment or subset i	ml
q_i	Radiotracer quantity in compartment or subset i	cps
C_i	Radiotracer concentration of compartment or subset i	cps/ml
$C_{art}^{H_2^{15}O}(t)$	Time-dependent concentration of $H_2^{15}O$ in arterial blood	cps/ml
$C_{art}^{O^{15}O}(t)$	Time-dependent concentration of $O^{15}O$ in arterial blood	cps/ml
λ_{H_2O}	Brain: blood partition coefficient for water	
λ	Brain: blood partition coefficient for water per unit weight	ml/100 g
R	Small vessel to large vessel hematocrit ratio	
F	Cerebral blood flow	ml/sec
PET_{calc}	Calculated tissue activity for PET	cts
PET_{obs}	Observed decay corrected tissue activity per unit weight	cts/100 g
CBF	Local cerebral blood flow	ml/sec·100 g*
CBV	Local cerebral blood volume	ml/100 g
$CMRO_2$	Local cerebral consumption rate of oxygen	ml/sec·100 g*
E	Local oxygen extraction	none

* More commonly ml/min·100 g for reporting actual values.

drainage at a concentration equal to the tissue concentration times the blood/brain partition coefficient for water. Except for additional input from extracted $O^{15}O$, this half of the model is identical to the classic one-compartment Kety model designed to measure blood flow (5).

To formulate the equations that describe these principles, we begin with the conservation equation (symbols in Table 1) for the second compartment containing $H_2^{15}O$,

$$V_2 \frac{dC_2}{dt} = \Phi_{in} - \Phi_{out}. \quad (1)$$

These fluxes are defined as:

$$\Phi_{in} = F \cdot \left(C_{art}^{H_2O}(t) + E \cdot C_{art}^{O_2}(t) \right) \quad (2)$$

and

$$\Phi_{out} = F \cdot C_2(t) / \lambda_{H_2O}. \quad (3)$$

Substituting these fluxes and integrating we can define $q_2(t)$, the quantity of $H_2^{15}O$ in Compartment 2, as:

$$q_2(t) = V_2 \cdot C_2(t) = F \cdot C_{art}^{H_2O}(t) * e^{-kt} + F \cdot E \cdot C_{art}^{O_2}(t) * e^{-kt}, \quad (4)$$

where $k = F / (V_2 \cdot \lambda_{H_2O})$ and "*" is the convolution operation. At implementation, however, k is calculated using conventional notation and the equivalent equation, $k = CBF / \lambda$.

We examine the $O^{15}O$ compartment by first assuming there are three subsets of this physical volume: precapillary (arterial), capillary, and postcapillary (venous). The concentration in the precapillary volume is set equal to the arterial $O^{15}O$ concentration. Since all oxygen extraction occurs in the capillary, we assume that the concentration in the postcapillary volume is arterial $O^{15}O$ concentration times the unextracted fraction. The capillary volume then is assumed to have a concentration equal to the average of the pre- and postcapillary volumes. Thus,

$$C_{pre}(t) = C_{art}^{O_2}(t), \quad (5)$$

$$C_{post}(t) = C_{art}^{O_2}(t) \cdot (1 - E) \quad (6)$$

and

$$C_{cap}(t) = C_{art}^{O_2}(t) \cdot (1 - 1/2E). \quad (7)$$

It follows that the quantity $q_1(t)$ of $O^{15}O$ in all blood compartments is

$$q_1(t) = V_1 \cdot C_1(t) = V_{pre} \cdot C_{pre}(t) + V_{cap} \cdot C_{cap}(t) + V_{post} \cdot C_{post}(t). \quad (8)$$

Since $V_1 = V_{pre} + V_{cap} + V_{post}$, we can make the fol-

lowing substitution for C_{pre} , C_{post} , and C_{cap} :

$$q_1(t) = V_1 \cdot C_1(t) = C_{art}^{O_2}(t) \cdot [V_1 - E(V_{post} + 1/2V_{cap})]. \quad (9)$$

With our two compartments thus analytically defined, we can then express the tissue time-activity curve that would be detected by an external device monitoring the contribution of both $O^{15}O$ and $H_2^{15}O$ as

$$q_{total}(t) = q_1(t) + q_2(t) \quad (10)$$

or

$$q_{total}(t) = C_{art}^{O_2}(t) \cdot [V_1 - E(V_{post} + 1/2V_{cap})] + F \cdot C_{art}^{H_2O}(t) * e^{-kt} + F \cdot E \cdot C_{art}^{O_2}(t) * e^{-kt}. \quad (11)$$

As mentioned above, the PET device cannot measure a cerebral time-activity curve, but rather the sum of all decay events between the start and stop of the scan. We express the predicted PET activity then as:

$$PET_{calc} = \int_{t_1}^{t_2} q_{total}(t) dt, \quad (12)$$

where t_1 and t_2 are the start and stop times, respectively. In detail,

$$PET_{calc} = (V_1 - E[V_{post} + 1/2V_{cap}]) \cdot \int_{t_1}^{t_2} C_{art}^{O_2}(t) dt + F \cdot \int_{t_1}^{t_2} C_{art}^{H_2O}(t) * e^{-kt} dt + F \cdot E \cdot \int_{t_1}^{t_2} C_{art}^{O_2}(t) * e^{-kt} dt. \quad (13)$$

Equation (13) is an explicit equation that predicts the total activity seen by the PET scan given the arterial blood curves for $O^{15}O$ and $H_2^{15}O$ following inhalation of $[O-15]oxygen$, the local blood flow, oxygen extraction, and blood volume. In practice, however, we measure the PET activity and calculate the extraction. The equation can be rewritten as:

$$E = \frac{PET_{calc} - F \cdot \int_{t_1}^{t_2} C_{art}^{H_2O}(t) * e^{-kt} dt - V_1 \cdot \int_{t_1}^{t_2} C_{art}^{O_2}(t) dt}{F \cdot \int_{t_1}^{t_2} C_{art}^{O_2}(t) * e^{-kt} dt - (V_{post} + 1/2V_{cap}) \cdot \int_{t_1}^{t_2} C_{art}^{O_2}(t) dt} \quad (14)$$

Since there is no current method to determine V_{post} and V_{cap} locally, we use literature values (6), where they are expressed as fractional parts of total blood volume. The values are found to be 0.83 and 0.01 for V_{post}/V_B and V_{cap}/V_B , respectively. After these numerical values have been inserted, the quantity CBV (cerebral blood flow) times R (where R is the ratio of small-vessel to large-vessel hematocrit), is substituted for V_B . Since $[O-15]oxygen$ is tightly bound to the cellular component of blood, the factor R is necessary to correct the CBV value for effects of hematocrit dilution that occur at the

tissue level (11). Note that in our calculation of CBV using Eq. (20), the term R appears in the denominator; thus the quantity $CBV \cdot R$ is actually independent of the value for R, since this term divides out.

Finally, substitution of CBF (cerebral blood flow) for F, and PET_{obs} for PET_{calc} gives the operational equation for the calculation of local oxygen extraction:

$$E = \frac{PET_{obs} - CBF \cdot \int_{t_1}^{t_2} C_{ari}^{H_2O}(t) \cdot e^{-kt} dt - CBV \cdot R \cdot \int_{t_1}^{t_2} C_{ari}^{O_2}(t) dt}{CBF \cdot \int_{t_1}^{t_2} C_{ari}^{O_2}(t) \cdot e^{-kt} dt - CBV \cdot R \cdot (0.835) \cdot \int_{t_1}^{t_2} C_{ari}^{O_2}(t) dt.} \quad (15)$$

Using E from the above equation, the local cerebral metabolic rate for O_2 ($CMRO_2$) is computed in the following manner:

$$CMRO_2 = E \cdot CBF \cdot C_aO_2, \quad (16)$$

where C_aO_2 is the total oxygen content of arterial blood.

Implementation of our mathematical model to calculate the local $CMRO_2$ and extraction requires the successful execution of several steps: (a) the adequate inhalation of $O^{15}O$ and subsequent PET scan of sufficient length to ensure statistical accuracy; (b) description of the $O^{15}O$ and $H_2^{15}O$ activity curves for arterial blood; (c) determination of blood flow and blood volume in all regions of interest; and (d) measurement of total arterial oxygen at time of the scan.

Simulations. The calculation of oxygen extraction and $CMRO_2$ is dependent on a number of factors. To understand the nature of this dependence, we used the final form of our oxygen model, Eqs. (15) and (16), in simulations designed to isolate and examine the error introduced by small errors in the measurement of CBV, CBF, PET-measured tissue activity, and recirculating water of metabolism.

In all simulations the same typical human arterial blood curves and blood oxygen content were used. The scan duration was 40 sec. The PET activity was not measured but calculated from Eq. (16) after assuming values for oxygen extraction.

To examine the effect of errors in the measurement of CBF, values were assumed for E (0.45) and CBV (4 ml/100 g), then the PET activity was calculated for a given $CMRO_2$. [Note that by Eq. (17), the fixing of $CMRO_2$, C_aO_2 , and E uniquely determines CBF]. Then, using the same value for PET activity, an error of +1% or +5% was introduced into the CBF term, and Eqs. (16) and (17) were used to calculate the new values for $CMRO_2$ and oxygen extraction. The values were compared with the original "true" values and the percent deviation was calculated. This process was performed

with $CMRO_2$ values of 1 to 6 ml/min·100 g (and CBF of 13.9 to 83.3 ml/min·100 g).

To examine the effect of errors in CBV, the above process was repeated with the exception that after the PET activity was calculated, the error was introduced in the CBV term. The range of $CMRO_2$ examined was again from 1 to 6 ml/min⁻¹·100 g. The simulation set had starting values for CBV of 4 and 6 ml/100 g, with the extraction value at 0.45.

To examine the effect of errors in the measurement of recirculating water, the PET activity was calculated after assuming values for CBV (4 ml/100 g), E (0.45), and a $CMRO_2$. Then the error of +5% was introduced in the recirculating water curve by increasing each instantaneous blood activity value. Using this new blood curve, the $CMRO_2$ and E were calculated and compared with the original values. The process was performed with $CMRO_2$ values from 1 to 6 ml/min·100 g. Additionally, the effect on $CMRO_2$ and E assuming no recirculating water of metabolism was simulated by zeroing all of $H_2^{15}O$ blood activity points. Ranges of CBF from 10 to 120 ml/min·100 g and E from 0.075 to 0.60 were examined.

To examine the effect of errors in the PET-measured tissue activity after inhalation of [O-15]oxygen, the above process was repeated with the exception that after the PET activity was calculated the 5% error was introduced in the PET_{obs} term. Using this new value for tissue activity, $CMRO_2$ was calculated and compared with its original value. The entire process was performed with $CMRO_2$ values of 1 to 6 ml/min·100 g and CBV values of 4 and 6 ml/100 g.

Implementation. The PETT VI system, a positron emission scanner, was used for all studies (7). Design and performance characteristics have been discussed (7,8). Studies were done in the low-resolution mode, giving an in-plane (transverse) resolution of 11.7 mm full width at half maximum (FWHM). Data were recorded simultaneously from seven slices, each with a 15.9-mm FWHM thickness and a center-to-center slice separation of 14.4 mm.

The PETT VI scan system does not correct for radioactive decay during data collection, so it is necessary to make such corrections in all reconstructed scan data from patients or phantoms. We use a method that assumes the underlying activity to be reasonably constant and that decay correction can be achieved with an "average" decay correction. This is computed as

$$\begin{aligned} \text{average decay} &= \int_0^T \frac{\exp(-\gamma T)}{T} dt \\ &= \frac{1 - \exp(-\gamma T)}{T \cdot \gamma}, \end{aligned} \quad (17)$$

where γ is the decay constant and T is the duration of the scan. Inversion of this average decay yields the decay-

correction factor. While it is true that the accuracy of this decay correction technique is dependent on the rate of change of the tissue activity during the scan, simulations can demonstrate that even for extreme examples the error introduced is quite small. For instance, in the case of an input of $H_2^{15}O$ by means of an instantaneous bolus injection and a rapid washout with tissue CBF = 100 ml/min·100 g, the error introduced by our method for a 40-sec scan, compared with on-line decay correction, is calculated to be 1.2%.

Calibration of the PETT VI system to permit expression of results in regional tissue activity is achieved by imaging a phantom containing various concentrations of C-11 bicarbonate. Aliquots from each of the six wedge-shaped chambers are counted in the same well counter used to count the blood samples. The observed counting rate is decay-corrected to the time the calibration scan begins, and is then multiplied by the duration of the scan. Results are expressed in counts/ml. Using a regression equation, the reconstructed regional data (PET counts/pixel) of the phantom are compared with the directly measured activity (counts/min). This relationship is used to calculate actual local tracer activities in tissue for scans obtained from animals and human subjects.

Our methods used to measure local CBF and CBV using PET are described elsewhere (9-11). For convenience of the reader, we have included a brief summary of these techniques.

For the measurement of regional CBF, a PET scan is performed following an intravenous bolus injection of 50-100 mCi of $H_2^{15}O$ contained in 12 ml of saline. Arterial blood samples are drawn every 5 sec until the end of the 40-sec scan. The PET scan is reconstructed and decay-corrected as described above.

The blood curve and scan data are analyzed according to general principles of inert-gas exchange developed by Kety (12) and later embodied in a tissue autoradiographic technique for the measurement of local brain blood flow in laboratory animals.(5). With this method, the local CBF is obtained by numerically solving the following equation for f , the flow per unit weight of tissue:

$$C_i(t) = fC_A(t) * \exp(-f/\lambda t), \quad (18)$$

where $C_i(t)$ is the local radiotracer concentration at time, t , derived from a quantitative autoradiogram of a brain slice; $C_A(t)$ is the measured concentration of radiotracer in arterial blood as a function of time; and λ is the brain:blood equilibrium partition coefficient for the tracer. The operation of convolution is denoted by the midline asterisk. PET scanners, including the one used in this study (7,8), do not have adequate sensitivity and temporal resolution to measure instantaneous tissue radioactivity, $C_i(t)$. Thus, to apply the autoradiographic

technique to in vivo human studies, a scan must be performed over many seconds, essentially summing the instantaneous tissue radioactivity over time. We have therefore modified the operational equation for this model (above) by an integration over the time of the scan ($t_1 - t_2$; 40 sec) as follows:

$$C = \int_{t_1}^{t_2} C_i(t) dt \\ = f \int_{t_1}^{t_2} C_A(t) * \exp(-f/\lambda t) dt, \quad (19)$$

where C is the local tissue activity measured by PET. A mean of gray- and white-matter values for the tracer partition coefficient for water in brain, equaling 0.95 is used (9,10). In order to establish the validity of this technique, we have measured local CBF with PET in adult baboons anesthetized with nitrous oxide and have compared it directly with cerebral blood flow measured in the same animal using injection of the internal carotid artery with O-15-labeled water and standard tracer principles (13,14). The details of these validation experiments are reported separately (10). The correlation between the PET-measured CBF and the true CBF was excellent. Over a blood flow range of 10-63 ml/min·100 g, $CBF(PET) = 0.90 CBF(true) + 0.40$ ($N = 23, r = 0.96, p < 0.001$). The slight underestimation of $CBF(true)$ by $CBF(PET)$ is due to the brain permeability limitation of O-15-labeled water. Because the brain permeability for water is less in the baboon than in humans (unpublished data) we believe that underestimation of CBF in data presented in this paper to be minimal, <5%.

Measurement of regional CBV with PET is accomplished with a technique previously developed in our laboratory (11). In the present application we have substituted $C^{15}O$ for ^{11}CO in the inhaled gas. After inhalation, 2 min are allowed for equilibration, then arterial blood is sampled every 30 sec until the end of a single 5-min PET scan. Blood volume expressed as ml/100 g, is calculated according to the following equation,

$$CBV = \frac{PET \cdot 100}{\int_{t_1}^{t_2} R \cdot D \cdot C_A(t) dt}, \quad (20)$$

where $C_A(t)$ is the decay-corrected radiotracer concentration in arterial blood, R is the mean ratio of the small-vessel to large-vessel hematocrit, equal to 0.85 (11), and D is the density of brain tissue, equal to 1.05 g/ml (15).

VALIDATION

In vivo validation of our method for the measurement of E with PET was accomplished by comparing two sequential measurements of the cerebral oxygen extraction

in baboons; the first using an intracarotid injection of $O^{15}O$ —a technique previously described (3) and validated (4)—and the second using our new PET technique.

The extraction of oxygen was measured in six adult baboons (*Papio papio*) weighing 18 to 25 kg. To facilitate the injection of small aliquots (~0.2 ml) of the baboon's blood containing $O^{15}O$ into the internal carotid artery, the baboons were anesthetized with phencyclidine (2 mg/kg) at least 2 wk before the experiment, and the right external carotid artery was ligated at its origin from the common carotid. At the time of experimentation the radiotracer was injected into the common carotid artery through a small catheter (0.021 cm i.d.) positioned there under fluoroscopic control.

For the actual comparison of our new PET method with the standard residue-detection technique using the intracarotid administration of oxygen-15-labeled blood (16) the baboons were anesthetized with ketamine (10 mg/kg), paralyzed with gallamine, intubated with a cuffed endotracheal tube, and passively ventilated on a gas mixture containing 70% nitrous oxide and 30% oxygen. The baboons were then positioned on a special couch that permitted placement of their heads in the PET VI imaging device or over a 3- by 2-in. NaI(Tl) detector appropriately collimated and located under the animal's head to ensure essentially uniform detection of a single cerebral hemisphere.

To permit the intracarotid injection of oxygen-15-labeled blood, a small catheter was percutaneously inserted into the femoral artery and its tip positioned in the right common carotid artery under fluoroscopic control. To prevent clotting in this arterial catheter system, which was used for the injection of radiotracer, monitoring of blood pressure, and sampling of arterial blood, all animals were heparinized at the beginning of the experiment. Arterial pH, P_{CO_2} , and P_{O_2} were measured before and after each injection or inhalation of radiotracer. To permit the intravenous injection of oxygen-15-labeled water, a small venous catheter was percutaneously placed in the femoral vein.

The head of the baboon was positioned with the aid of a vertical laser line such that the center of the lowest slice corresponded to a line running transversely through the center of the cerebral hemispheres. A lateral skull radiograph with this line marked by a vertical radiopaque wire provided a record of the position of the lowest PET slice. Because of the size of the adult baboon brain (~150 g), only data from this bottom slice and corresponding to the hemisphere studied with the intracarotid injection of oxygen-15-labeled water (see above) were used in these experiments. Attenuation correction was determined for each animal by obtaining a transmission scan using a ring source of activity (germanium-68) fitted to the PET VI tomograph as previously described (7).

The signal from the single NaI(Tl) detector was processed by a pulse-height discriminator with a 481- to 541-keV energy window to reduce scattered radiation. The accepted counts were stored in a small laboratory computer, which processed these data including corrections for electronic dead time loss, physical decay (O^{15} half-life = 123 sec), and background, conversion to count rate as a function of time, and readout by x-y plotter. Temporal resolution was achieved in the initial portion by 0.1-sec sampling. Enough activity was injected into the carotid to provide count rates of 10,000–20,000 cps, ensuring adequately smooth recordings.

By altering the respiratory rate and thus the arterial carbon dioxide tension, the CBF, E, and $CMRO_2$ were varied to achieve as broad a range of E as possible. At least 20 min were allowed between changes in the respiratory rate to permit a new steady state to be achieved. Measurements of arterial blood gases bracketed all measurements of CBF, E, and $CMRO_2$.

The PET-measured value for oxygen extraction was obtained from the mean of a rectangular region of interest (7.3 cm²) placed over the area corresponding to the right hemisphere on the PET [O^{15}] oxygen scan after pixel-by-pixel processing had been done to show oxygen extraction. The placement of the region, aided by the lateral skull film and the transmission image, was not critical, since oxygen extraction was seen to be remarkably uniform across the baboon brain.

Human studies. For human studies a 20-gauge plastic catheter was placed in the radial artery under local anesthesia. The head was positioned with the aid of a vertical laser line such that the lowest slice corresponded to the patient's orbito-meatal line. A lateral skull radiograph with the line marked by a vertical radiopaque bar provided a record of the head position. A molded face mask placed just before the lateral skull radiograph provided immobilization of the head during the scan; it can also enable accurate repositioning in subjects if follow-up studies are required.

After the head was positioned and immobilized, a transmission scan was performed with a ring phantom containing Ge-68. This provided for attenuation correction for quantitative reconstruction of subsequent scans, and a means of identifying the bony limits of the calvarium for the computation of whole-slice and hemisphere-average metabolic rates and blood flow.

Oxygen-15 O_2 was administered by inhalation. To accomplish this, cyclotron-produced $O^{15}O$ diluted with nitrogen (N_2) was pumped into a lead-shielded rubber air bag at the patient's side. When sufficient activity was collected, the patient inhaled the gas (~40–80 mCi) through a short plastic ventilator hose. Scanning began immediately after adequate inhalation of the $O^{15}O$, and lasted 40 sec. Time zero ($t = 0$) was defined as the time inhalation of $O^{15}O$ commenced.

Concurrent with the inhalation of $O^{15}O$, blood sampling began at a rate of 0.5 ml every 4 to 5 sec and continued throughout the scan. Samples were collected in preweighed, 3-ml syringes. Total oxygen-15 activity was measured with a calibrated well counter. Actual volume collected was calculated from the difference between syringe's dry and wet weights. The density for blood was assumed to be 1.05 g/ml. All samples were corrected for radioactive decay ($T_{1/2} = 123$ sec) back to the zero time, and results expressed in cps/ml blood.

At the end of the PET scan, a 3-ml arterial blood sample was collected; of this, 0.5 ml was counted as above, 1 ml sent for measurement of oxygen content, and the remainder fractionated using an Eppendorf high-speed centrifuge for 30 sec. The resulting plasma supernatant was pipetted off, and 0.5 ml was placed in a 3-ml preweighed syringe and counted as above in the well counter. After correction for radioactive decay, the results were expressed in cps/ml plasma.

We assume that all $O^{15}O$ in blood exists bound to hemoglobin in the red blood cells. The plasma activity can then be considered pure $H_2^{15}O$ activity. To rule out lysis of red cells and the resultant release of hemoglobin into the plasma, hemoglobin determinations were performed on all plasma samples using a technique sensitive to very small hemoglobin concentrations (17). The $H_2^{15}O$ contribution to the total blood activity is then calculated as $C_{art}^{H_2O} = C_{pl} \cdot FWC_{bl} / FWC_{pl}$, where C_{pl} is the plasma activity, FWC_{bl} is the fractional water content of blood, and FWC_{pl} is the fractional water content of plasma. Values of 0.80 g/g-blood and 0.92 g/g-plasma were used for the water contents of whole blood and plasma, respectively (18).

We describe the amount of recirculating $H_2^{15}O$ of metabolism in blood from zero time, when there is no $H_2^{15}O$, to the time of the measured value of $C_{art}^{H_2O}$ (from the fractionated blood sample), by linear interpolation. This results in an estimate of $C_{art}^{H_2O}$ for each sample drawn for total blood activity. Subtraction of these interpolated values from the total blood activity gives the estimated $C_{art}^{O_2}$ values.

As an alternative to the method of single fractionation and linear interpolation described above, we have also measured the $C_{art}^{H_2O}$ curve explicitly in selected subjects from whom 3-ml samples were drawn every 10 sec. Fractionation and counting were performed as above. Resultant activity curves were expressed as individual activity for $H_2^{15}O$ of metabolism and $O^{15}O$.

Calculation of $CMRO_2$ and E requires local CBF and CBV values. These were obtained from two additional, successive PET scans as described above. Intervening movement of the head was prevented by the face mask (see above). The complete study, with three PET scans, was performed in ~ 30 min. Arterial blood gases were obtained with each scan.

To obtain time-activity curves for arterial blood, we

draw samples from the radial artery (rarely from the femoral, when our study is preceded by arteriography). Radial blood incurs a small time delay, however, relative to cerebral blood, because of the radial artery's greater distance from the heart. Since the accuracy of our techniques is likely to be affected by such differences, we correct for them in our human studies, determining the arrival time in the head of the subject by observing and recording the time of an abrupt increase in the coincidence counting rate of PETT VI (sampling from a single bank pair once every second) and the arrival time at the peripheral sampling site from the arterial time-activity curve. The latter curve is then shifted to correct for the indicated delay.

Estimates of the $CMRO_2$ for the cerebral hemispheres of our normal, young-adult subjects represent the mean and standard deviation of values for these parameters in all pixels in the top four PET scan slices. The attenuation scan (see above) was used in each case to mask these slices in order to exclude all activity outside the calvarium. Estimates of the $CMRO_2$ for the cerebellar hemispheres in these same subjects was based on a region of interest 19×19 mm in the horizontal plane and ~ 13 mm thick, centered over each cerebellar hemisphere (total volume of these samples was approximately 4.7 cm^3).*

RESULTS

Simulations of errors in E and $CMRO_2$ imposed by error in the measurement of CBV are shown in Fig. 2. At low metabolic rates ($CMRO_2 = 1.5$ ml/min·100 g, $E = 0.45$), a +5% error in CBV ($CBV = 6.0$ ml/100 g) results in a -10.2% error in $CMRO_2$ and E . At higher metabolic rates ($CMRO_2 = 6$ ml/min·100 g) the same error in CBV results in a much smaller percent error,

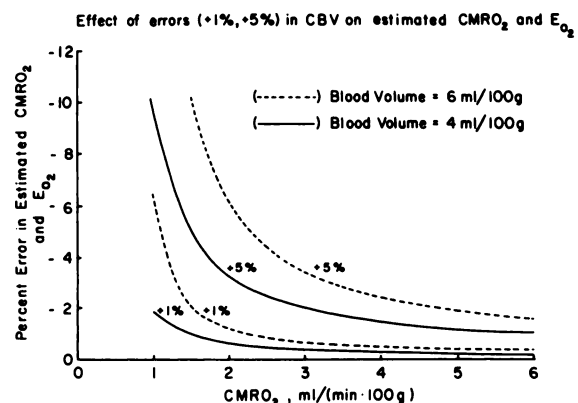


FIG. 2. Predicted errors in brain oxygen extraction (EO_2) and cerebral utilization rate for oxygen ($CMRO_2$) determined for small errors (1% and 5%) in measured cerebral blood volume (CBV), using Eqs. (16) and (17) of text. Initial values of 4 and 6 ml/100 g were assumed for CBV. Results demonstrate that estimates of E and $CMRO_2$ are more sensitive to errors in CBV at higher CBV values and lower values of $CMRO_2$.

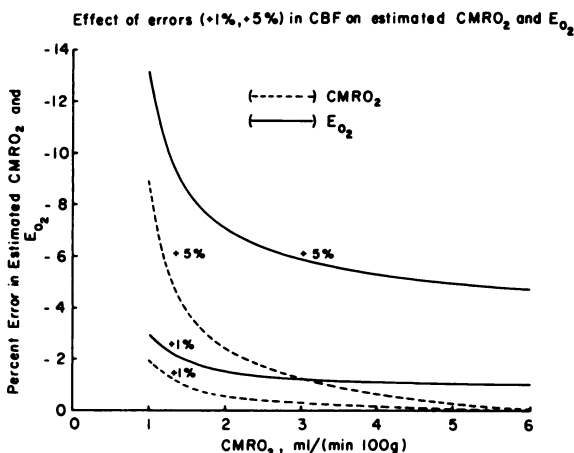


FIG. 3. Predicted errors in brain oxygen extraction (E_{O_2}) and cerebral utilization rate for oxygen ($CMRO_2$) determined for small errors (1% and 5%) in measured cerebral blood flow (CBF) using Eqs. (16) and (17) of text. Results demonstrate that E (solid lines) is more sensitive than $CMRO_2$ (dashed lines) to errors in CBF. For both E and $CMRO_2$, sensitivity to errors in CBF increased at lower values of $CMRO_2$.

-1.6%. Additionally, simulations showed that as CBV increases, there is a concordant increase in $CMRO_2$ error for the same percent error in CBV measurement.

Simulations of errors in E and $CMRO_2$ imposed by errors in the measurement of CBF demonstrated a dramatic difference in the predicted error in $CMRO_2$ compared with E (Fig. 3). At all levels of oxygen metabolism, E is much more sensitive than $CMRO_2$ to errors in CBF. This is most dramatic at high metabolism ($CMRO_2 = 6 \text{ ml/min}\cdot 100 \text{ g}$), where a +5% error in CBF produced a -4.7% error in E but only +0.01% error in $CMRO_2$. As with CBV, errors in CBF had less affect on both $CMRO_2$ and E as metabolism increased.

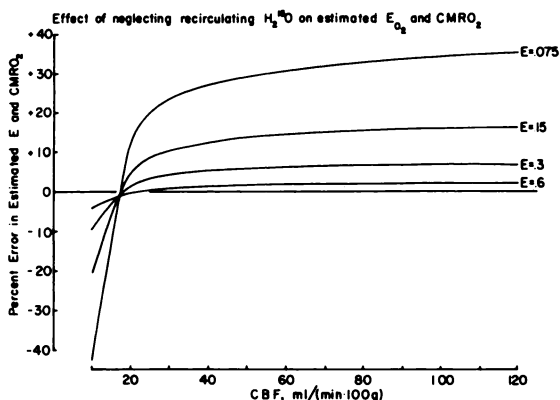


FIG. 4. Predicted errors in oxygen extraction (E_{O_2}) and cerebral utilization rate for oxygen ($CMRO_2$) were determined neglecting recirculating $H_2^{15}O$ of metabolism using Eqs. (16) and (17) of text. Errors were calculated over large range of E (0.075 to 0.6) and CBF (10-120 ml/min-100 g). Results demonstrate minimal errors in $CMRO_2$ and E at higher values of E . At low values of E , error introduced by ignoring recirculating water is considerable at nearly all values of CBF examined.

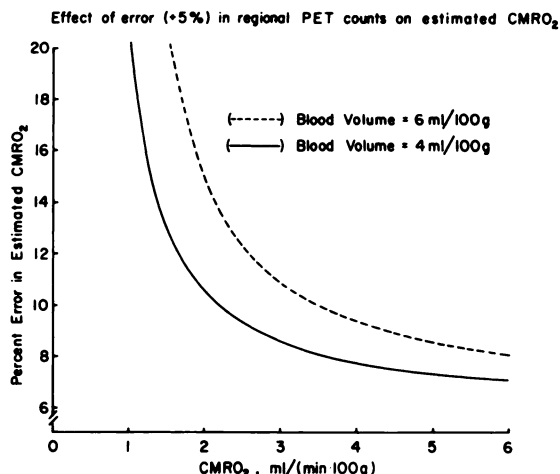


FIG. 5. Predicted errors in cerebral utilization rate of oxygen ($CMRO_2$) determined for +5% errors in regional PET counts from $O^{15}O$ scan using Eqs. (16) and (17) of text. Results demonstrate higher sensitivity of oxygen model to errors in PET-measured tissue activity at low $CMRO_2$ values and high CBV values.

Simulations of our model's sensitivity to the presence of recirculating water of metabolism are shown in Fig. 4. These data indicate that ignoring recirculating $H_2^{15}O$ of metabolism leads to errors in the calculation of $CMRO_2$ and E that are dependent upon the true E and the CBF. As might be anticipated, large errors in estimated E and $CMRO_2$ occur when CBF is elevated and true E is reduced. Simulations done with the introduction of a 5% error into the measurement of recirculating water led to less than a 1% error in $CMRO_2$ at all $CMRO_2$ values examined.

Simulations of errors in $CMRO_2$ imposed by error in regional PET-measured tissue activity are shown in Fig. 5. At low metabolic rates ($CMRO_2 = 1.5 \text{ ml/min}\cdot 100 \text{ g}$, $E = 0.45$) a 5% error in PET counts results in a 13% error in $CMRO_2$ when CBV equals 4 ml/100 g, and a

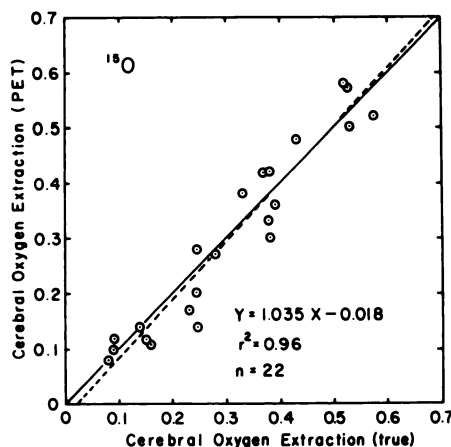


FIG. 6. Comparison of oxygen extraction (E) in baboons measured by intracarotid injection of $O^{15}O$ (true) and by our PET method. Twenty-two sequential measurements of E were done in six animals over a range of 0.08 to 0.58. Results show close correlation (dashed line) that is not statistically different from unity (solid line).

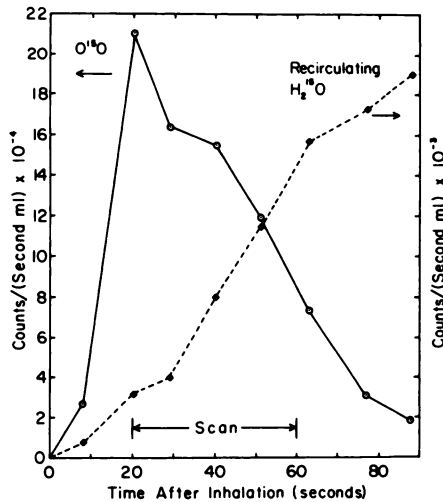


FIG. 7. Typical fractionated (i.e. $O^{15}O$ and $H_2^{15}O$ water of metabolism) arterial blood curves in human subject following inhalation of ~ 50 mCi of O-15 oxygen. Note factor of ten difference in scale between left ($O^{15}O$) and right ($H_2^{15}O$) axes. Recirculating $H_2^{15}O$ of metabolism is only 6% of total cumulative blood activity during 40-sec PET scan. At $t = 90$ sec, fraction of $H_2^{15}O$ water of metabolism is 50%. All activities have been decay-corrected to zero time.

21% error when CBV equals 6 ml/100 g. Importantly, these errors are reduced at normal to high metabolic rates. For a $CMRO_2$ equal to 6 ml/min-100 g the errors introduced by a 5% error in PET counts are only 7% and 8% for the low and high CBV values, respectively.

The validation experiments in baboons yielded 22 pairs of extraction values, shown in Fig. 6, with a range of E from 0.08 to 0.58. Linear regression analysis of these

points resulted in the equation: $E(PET) = 1.035 \cdot E(true) - 0.018$ ($r^2 = 0.958$, $N = 22$). This line is not significantly different from unity. Additionally, visual inspection gives no evidence that the E(PET) values deviate systematically at either high or low extractions.

Inhalation of approximately 50 mCi of $O^{15}O$ by a human subject resulted in the blood activity curves shown in Fig. 7, where fractionated samples were obtained for $O^{15}O$ and $H_2^{15}O$ activity. Soon after the termination of the 40-sec scan, the fraction of total blood activity existing as recirculating $H_2^{15}O$ of metabolism was 18%.

A typical study in a normal human is shown in Fig. 8. Numbered regions of interest have been placed over various areas of gray and white matter, with the measured $CMRO_2$ printed below each image. In this subject these values ranged from 2.12 ml/min-100 g for white matter, to 4.51 ml/min-100 g for gray matter. The average $CMRO_2$ for the cerebral hemispheres of five such normal subjects (ages 23 to 40) was 2.93 ± 0.37 (s.d.) ml/min-100 g. In this same group of subjects the average $CMRO_2$ of the cerebellar hemispheres was 3.65 ± 0.60 ml/min-100 g. Side-to-side differences in the $CMRO_2$ were less than 1% in both cerebral and cerebellar hemispheres.

DISCUSSION

An advantage of our oxygen metabolism model is its simplicity and relative lack of limiting assumptions. The local CBF, which determines the entrance and exit behavior of the only metabolite, $H_2^{15}O$, is measured ex-

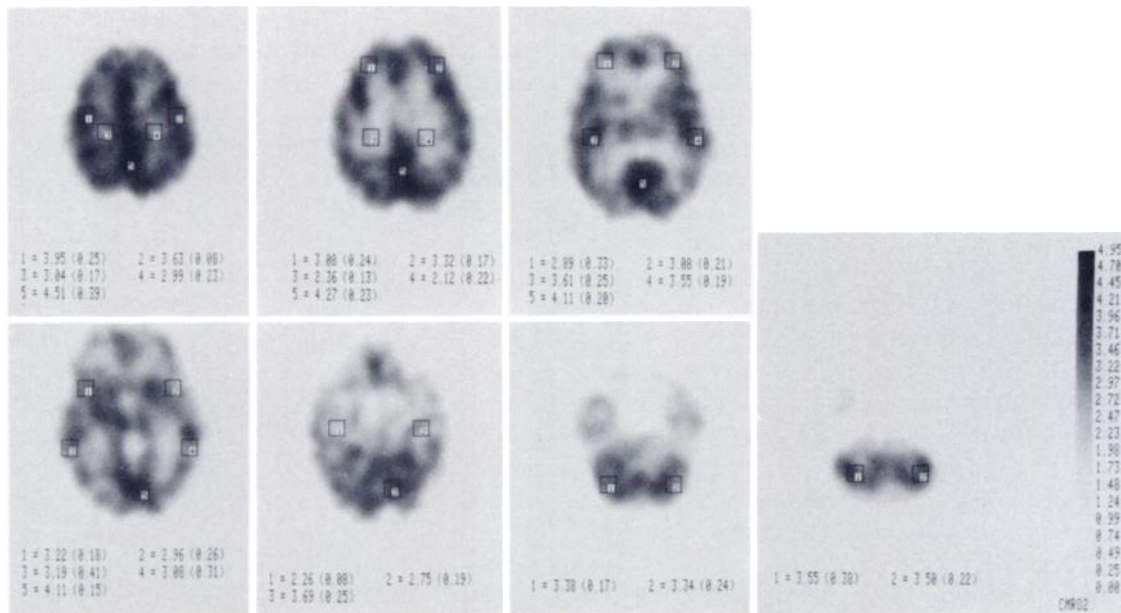


FIG. 8. Typical quantitative measurement of $CMRO_2$ in normal male subject, age 23. PET-scan data were collected over 40 sec. Quantitative gray scale was set to same maximum of 4.95 ml/min-100 g for each slice to permit more accurate visual comparison. Specific regions have been selected in each slice to illustrate local variations in cerebral metabolic rate for oxygen ($CMRO_2$). Values for these regions are listed below each slice along with standard deviation for 25 pixels in each region.

plicity. Since no average value is assumed for local flow, the model is equally useful in varying areas of high, normal, or low blood flow. The local CBV, which is necessary for determining the amount of $O^{15}O$ tracer in the vascular compartment, is also measured explicitly, resulting in similar versatility. Recirculating water of metabolism, contributing to the overall arterial-blood activity curve, is measured explicitly. Thus, few assumptions are made regarding the subject's general metabolic rate or physiology as it pertains to these variables.

The relative distribution of the CBV in precapillary, capillary, and postcapillary sections is assumed to be constant regardless of the total blood volume. While there are no literature data disputing or confirming this assumption, it is intuitive that a region including part of a cerebral venous sinus would have a postcapillary blood fraction above the average. This is not felt to be a serious limitation to the model, since the postcapillary fraction is estimated at 0.83 and at most would theoretically increase to 1.0 if the entire region was in a venous sinus. The measurement of $CMRO_2$ in such an uninteresting region would have minimal importance.

An additional assumption regarding the segments of the blood volume is that they are in constant equilibrium with each other. In other words, the arterial blood entering a given region will instantaneously affect the precapillary, capillary, and postcapillary divisions. Obviously, this differs from reality where the arterial blood affects the precapillary volume, which in turn affects the capillary volume, which in turn affects the postcapillary volume. The time course of these events is dependent on the actual volumes involved and the blood flow rate. To model this additional concept, one to two compartments would need to be added and the equations increased in complexity by at least two more convolution operations. However, the actual time-activity curves of the blood compartment are not used in the calculation of oxygen extraction and $CMRO_2$; rather, the time integrals of the blood activity over the length of the scan are used. We feel this greatly diminishes the difference between the two methods. Further work may be needed to verify this assumption, with consideration of both normal and abnormal blood flows and blood volumes.

Inherent in the model's structure is the assumption that no molecular oxygen exists outside the vascular compartment. Clearly, some must exist in the tissue or there could be no metabolism. However, the absolute value of this tissue oxygen concentration has been found to be very low (19,20), essentially negligible relative to the vascular oxygen source.

The validation study using monkeys, sequentially studied by the intracarotid injection technique and then with the PET scan, demonstrated a very close correlation. Of the original 28 sets of data, corresponding to 84 PET scans, a total of six sets were removed from final

analysis. Three sets were removed because the monkey involved developed a clinically obvious cerebral infarct subsequent to the study. Three other sets were removed due to technically poor blood-activity curves in one of the three scans for each set. Even when we considered all data sets, linear regression analysis yielded a close correlation between the two methods, and was not significantly different from unity.

The purpose of the simulations was to identify the conditions that adversely affected the accuracy of our model. No attempt was made to exhaust all possibilities, but the major variables measured externally—local CBF, blood volume, recirculating water of metabolism, and PET-measured tissue activity—were included. The results demonstrate that estimates of $CMRO_2$ and E are not critically dependent on the accuracy of the first three variables. However, it is equally apparent that a mere global estimate for blood flow and blood volume could lead to dramatic errors, as these variables can vary two- to threefold across the various regions of the brain. An error in the quantity of recirculating water seems to have much less impact on the final estimates of oxygen extraction and $CMRO_2$. The assumption of no recirculating water, however, may lead to considerable error in $CMRO_2$ and E. While no attempt was made to calculate the precision of our $CMRO_2$ measurements in human subjects, simulations demonstrated that errors in PET-measured tissue activity resulted in significant errors in the $CMRO_2$ and E values. Additionally, all simulations indicated that areas of the brain with high $CMRO_2$ had the lowest errors. Gray matter, with its superior average metabolic rate, would fall into this category.

Some caution must be observed in comparing our preliminary cerebral hemisphere values for the $CMRO_2$ for normal young adults, with measurements in the literature. Our value of 2.93 ml/min·100 g is slightly lower than that reported by others using the standard Kety technique (21,22) or our own results using residue detection and O-15-labeled radiopharmaceuticals injected into the internal carotid artery (23). This difference is probably due to partial-volume averaging. By demarcating the cerebral hemispheres as all activity lying within the outer table of the skull (see Methods, Human studies), we obviously include cerebrospinal fluid spaces surrounding the brain and the brain ventricular system. Percent estimates of these spaces in normals (24) indicate they represent ~10% of the volume of the cranial cavity. Assuming such a volume for our subjects, we would correct our value for the cerebral hemispheres to 3.22 ml/min·100 g. We have obviously ignored the contribution from bone in this estimate of the true $CMRO_2$ for the cerebral hemispheres. Preliminary studies (unpublished) indicate that the calvarium may represent 20% of the area sampled in these measurements. If so, the true average $CMRO_2$ for young adults, using our method with PET, will be more like 3.90

ml/min·100 g. It is of interest, in this regard, that our value for the CMRO₂ of the cerebellum, based on a region of interest placed *within* each cerebellar hemisphere, is considerably higher than that we obtain for the cerebral hemispheres (i.e. 3.65 ± 0.60 compared with 2.93 ± 0.37 ml/min·100 g). We explain this difference primarily as due to exclusion of fluid and bone. In performing our validation studies in baboons (Fig. 6) we used a region of interest placed within the cerebral hemisphere to avoid this problem. Where measurements of global hemisphere metabolic rates as well as other parameters are of interest to investigator, explicit corrections will be necessary to avoid partial-volume effects. The strategy of Gado et al. (24) is a convenient approach to this problem.

Our implementation of these PET scan techniques for measuring regional CMRO₂, cerebral blood flow, and cerebral blood volume has been rewarding. The use of short-lived oxygen-15 permits the three sequential scans, each following an administration of H₂¹⁵O, C¹⁵O, or O¹⁵O, to be accomplished within half an hour. Reliability of the results is supported by simulations and validation studies. The versatility of the technique should permit experimental design to include a broad range of normal and abnormal states.

FOOTNOTE

These studies were approved by the Human Studies Committee and the Radioactive Drug Research Committee (United States Food and Drug Administration) of the Washington University School of Medicine. Informed consent was obtained from each subject before PET scanning.

ACKNOWLEDGMENTS

This research was supported by NIH Grants NS 06833, NS 14834, and HL 13851. Dr. Herscovitch and Martin were Fellows of the Medical Research Council of Canada.

REFERENCES

1. SUBRAMANYAN R, ALPERT NM, HOOP B JR, et al: A model for regional cerebral oxygen distribution during continuous inhalation of ¹⁵O₂, C¹⁵O and C¹⁵O₂. *J Nucl Med* 19:48-53, 1978
2. FRACKOWIAK RSJ, LENZI G, JONES T, et al: Quantitative measurement of regional cerebral blood flow and oxygen metabolism in man using ¹⁵O and positron emission tomography: Theory, procedure and normal values. *J Comput Assist Tomogr* 4:727-736, 1980
3. TER-POGOSSIAN MM, EICHLING JO, DAVIS DO, et al: The measure in vivo of regional cerebral oxygen utilization by means of oxyhemoglobin labeled with radioactive oxygen-15. *J Clin Invest* 49:381-391, 1970
4. RAICHLER ME, GRUBB RL JR, EICHLING JO, et al: Measurement of brain oxygen utilization with radioactive oxygen-15: experimental verification. *J Appl Physiol* 40:638-640, 1976
5. KETY SS: Measurement of local blood flow by the exchange of an inert, diffusible substance. *Meth Med Res* 8:228-236, 1960
6. RUSHMER RF: *Cardiovascular Dynamics*. Fourth Edition. Philadelphia, W.B. Saunders Company, 1976, p 8, figure 1-3
7. TER-POGOSSIAN MM, FICKE DC, HOOD JT, et al: PETT VI: A positron emission tomography utilizing cesium fluoride scintillation detectors. *J Comput Assist Tomogr* 6:125-133, 1982
8. YAMAMOTO MM, FICKE DC, TER-POGOSSIAN MM: Performance study of PETT VI, a positron computed tomograph with 288 cesium fluoride detectors. *IEEE Trans Nucl Sci* NS-29:529-533, 1982
9. HERSCOVITCH P, MARKHAM J, RAICHLER ME: Brain blood flow measured with intravenous H₂¹⁵O. I. Theory and error analysis. *J Nucl Med* 24:782-789, 1983
10. RAICHLER ME, MARTIN WRW, HERSCOVITCH P, et al: Brain blood flow measured with intravenous H₂¹⁵O. II. Implementation and validation. *J Nucl Med* 24:790-798, 1983
11. GRUBB RJ JR, RAICHLER ME, HIGGINS CS, et al: Measurement of regional cerebral blood volume by emission tomography. *Ann Neurol* 4:322-328, 1978
12. KETY SS: The theory and application of the exchange of inert gas at the lungs and tissues. *Pharmacol Rev* 3:1-41, 1951
13. EICHLING JO, RAICHLER ME, GRUBB RL JR, et al: Evidence of the limitations of water as a freely diffusible tracer in brain of the Rhesus monkey. *Circ Res* 35:358-364, 1974
14. RAICHLER ME, EICHLING JO, STRAATMANN MD, et al: Blood brain barrier permeability of ¹¹C-labeled alcohols and ¹⁵O-labeled water. *Am J Physiol* 230:543-552, 1976
15. TORACK RM, ALCALA H, GADO M, et al: Correlative assay of computerized cranial tomography (CCT), water content and specific gravity in normal and pathological postmortem brain. *J Neuropath Exp Neurol* 35:385-392, 1976
16. WELCH MJ, TER-POGOSSIAN MM: Preparation of short half-lived radioactive gases for medical studies. *Radiation Res* 36:580-587, 1968
17. SONNENWIRTH AC, JARETT L, eds: *Gradwohl's Clinical Laboratory Methods and Diagnoses*. 8th Edition. St. Louis, MO, C.V. Mosby Company, 1980, Part III, pp 886-888
18. DAVIS FE, KENYON K, KIRK J: A rapid titrimetric method for determining the water content of human blood. *Science* 118:276-277, 1953
19. DANFIELD RA, NAIR P, WHALEN WJ: Mass transfer, storage and utilization of O₂ in cat cerebral cortex. *Am J Physiol* 219:814-821, 1970
20. METZGER H, HEUBER S: Local oxygen tension and spike activity of the cerebral grey matter of the rat and its response to short intervals of O₂ deficiency or CO₂ excess. *Pflugers Arch* 370:201-209, 1977
21. KETY SS, SCHMIDT CF: The nitrous oxide method for the quantitative determination of cerebral blood flow in man: Theory, procedure and normal values. *J Clin Invest* 27:476-483, 1948
22. KETY SS, SCHMIDT CF: The effects of altered arterial tensions of carbon dioxide and oxygen on cerebral blood flow and oxygen consumption of normal young men. *J Clin Invest* 27:484-492, 1948
23. CARTER CC, EICHLING JO, DAVIS DO, et al: Correlation of regional cerebral blood flow with regional oxygen uptake using ¹⁵O method. *Neurology* 22:755-762, 1972
24. GADO M, HUGHES CP, DANZIGER W, et al: Volumetric measurements of the cerebrospinal fluid spaces in demented subjects and controls. *Radiology* 144:535-538, 1982